Nanoparticle Assembly

DOI: 10.1002/anie.200901621

One-Dimensional Gold Nanoparticle Arrays by Electrostatically Directed Organization Using Polypeptide Self-Assembly**

Nikhil Sharma, Ayben Top, Kristi L. Kiick, and Darrin J. Pochan**

The study of interactions between particles organized in a linear configuration is interesting from a quantum mechanical perspective, and the anisotropic properties of linear assemblies is of potential interest for the development of solid-state devices.[1–3] This anisotropy may be manifested as a difference in the magnetization and coercivity obtained in a magnetic-nanoparticle array when a field is applied along the chain or orthogonal to it.[4,5] Nonlinear electrical characteristics[3] or dichroism in the optical spectra with longitudinal and transverse polarizations of light[6,7] in metal nanoparticle arrays are other examples of such anisotropy, and the construction of such arrays would offer opportunities in multiple applications. Engineering matter at submicron length scales has been an area largely dominated by top-down methodologies. Control of interparticle spacing in metal-nanoparticle arrays by using techniques such as electron beam lithography has been found to have a dramatic impact on the optical response of the nanoparticle assembly,[8–10] and has implications in fields such as plasmonics[11] and energy transport.[12,13] The use of templates such as carbon nanotubes[14] and linear pores[15] to construct one-dimensional nanostructures has been demonstrated previously. In addition, polymers have recently begun to play an increasingly active role as elements that can reproducibly direct the arrangement of nanoparticles into functional geometries.[16,17] Self assembling systems offer convenient yet powerful bottom–up strategies for the creation of nanostructures that can be deployed in the realization of functional nanoscale devices.[18,19]

The utilization of biomolecules such as DNA,[3,20–24] and protein-based materials[25–27] or viruses[28,29] to dictate the organization of nanoparticles has been shown to be an effective and robust paradigm. The use of peptide-based structures[30,31] in nanotechnology confers numerous advantages such as the specification of assembled nanostructure by changes in the primary sequence of the peptide, as well as the adoption of various hierarchical morphologies in solution.[32–35] This approach consequently permits the engineering of chemical functionality at precise positions in the nanoarchitecture of the assembled morphology. This functionality can be highly selective toward the binding of different inorganic materials[36] and may be engineered for biological recognition.[37] Herein, we demonstrate the construction of one-dimensional gold nanoparticle arrays with precise axial separations using self-assembling polypeptide fibrils. We elucidate the self-assembly of an alanine-rich polypeptide (designated 17H6) into fibrils that present regularly spaced charged patches along the fibril length. These positively charged patches are then utilized for the electrostatic binding of oppositely charged inorganic nanoparticles, thus resulting in linear nanoparticle arrays. The nanoparticles are immobilized on the fibril template at a well-defined and periodic spacing that is commensurate with the charged patch separation predicted from the self-assembly model described for the template polypeptide.

Electrostatically directed nanoparticle assembly[22,38] offers advantages such as simplicity of design and high yields. In addition, the modular nature of electrostatic nanoparticle organization allows the possibility of assembling different types of nanoparticles onto the fibril simply by manipulating the ligand that covers the particle surface so that it bears the appropriate charge. Organization of nanoparticles using polypeptide templates represents a robust yet flexible bottom–up nanofabrication method. Precedents of peptide-templated[30,37,39–43] nanoparticle assembly have established the feasibility of designing interactions between inorganic nanoparticles and peptide-based nanostructures; herein we demonstrate a fine degree of control over the relative placement of individual nanoparticles. Importantly, the molecular system described here can potentially be employed for controlling axial inter-nanoparticle spacing from an exclusively bottom–up perspective through systematic changes in the polypeptide primary sequence (see below).

The recombinant polypeptide 17H6 [MGH_{10}SSGHIHM $(AAAQEAAAAQAAAQAEAAQAAQ)_6$AGGYGGMG] was expressed from an *E. coli* expression host and purified by metal chelate affinity chromatography, as described previ-

[*] N. Sharma, A. Top, Prof. K. L. Kiick, Prof. D. J. Pochan
Department of Materials Science & Engineering
University of Delaware
201 DuPont Hall, Newark, DE 19716 (USA)
Fax: (+1) 302-831-4545
E-mail: kiick@udel.edu
pochan@udel.edu

[**] This work was supported in part by the National Institutes of Health (1-R01-EB006006-01), the National Center for Research Resources (1-P20-RR017716-01; a component of the National Institutes of Health), and the US Department of Defense (ARL CMR Pochan (CCMT332157)). We acknowledge the W. M. Keck foundation for partial funding of the College of Engineering Electron Microscopy Lab at the University of Delaware. A portion of this work was performed at the DuPont–Northwestern–Dow Collaborative Access Team (DND-CAT) located at Sector 5 of the Advanced Photon Source (APS). DND-CAT is supported by E.I. DuPont de Nemours & Co., The Dow Chemical Company, and the State of Illinois. Use of the APS was supported by the U.S. Department of Energy, Office of Science, Office of Basic Energy Sciences, under contract no. DE-AC02-06CH11357. We acknowledge the support of Dr. Honggang Cui for X-ray data acquisition and Dr. Kirk Czymmek for assistance with the congo red assay.

Supporting information for this article is available on the WWW under http://dx.doi.org/10.1002/anie.200901621.

ously.[44,45] The assembled nanostructure of 17H6 is strongly dependent on its microenvironment, and can be controlled by changes in the initial solution conditions, in which the assembly is conducted, particularly pH and temperature. At neutral pH, the polypeptide adopts a helical, non-aggregated structure. At acidic pH and ambient temperatures, aggregates of controlled size, with individual molecules that maintain a helical structure, are observed.[45] However, in an acidic environment (pH 2.3) and at elevated temperatures, the polypeptide assembles into stable, micrometer-long fibrils of monodisperse width. Circular dichroic spectroscopy (CD) studies indicated that the temperature-induced conversion of the secondary structure of the polypeptide to β sheet occurred at pH 2.3 and 80 °C, which suggests that the fibrils arose from β-sheet assembly.[45] The fibril formation was found to be irreversible as the temperature was lowered, and fibrils subsequently remained stable throughout further processing and characterization.[45] 17H6 fibrils were imaged by transmission electron microscopy (TEM) for characterization of their physical dimensions. Figure 1a shows a bright field (BF)

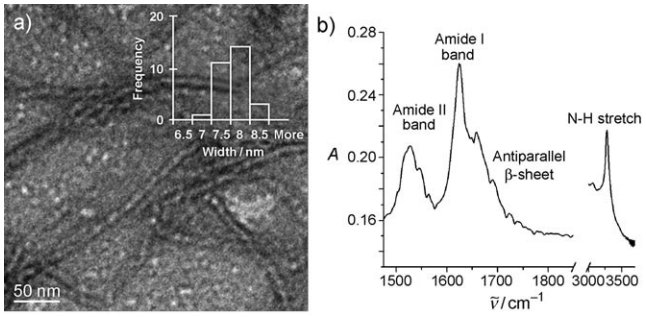

Figure 1. a) TEM image of 17H6 peptide fibrils stained with uranyl acetate. The fibril width distribution chart is shown as inset; b) FTIR spectrum of 17H6 fibrils.

TEM image of the fibrils stained with uranyl acetate. Fibrils were observed that spanned microns in length and possessed a monodisperse width. A frequency distribution chart for the fibril widths shows a narrow fibril width distribution centered at (7.6 ± 0.4) nm (Figure 1a, inset). Instances of lateral aggregation or branching of fibrils were not observed.

The β-sheet conformation suggested by the CD data[45] was corroborated by wide-angle X-ray scattering (WAXS; Figure S1 in the Supporting Information). The WAXS spectrum shows a broad peak with maximum at $2\theta = 10.4°$, which corresponds to a d-spacing of 4.56 Å and is consistent with the reported repeat spacing between adjacent sheets in the β-sheet conformation for peptides.[46] Similarly, in the FTIR spectrum (Figure 1b), peaks at 1624, 1528, and 3279 cm^{-1} correspond to amide I, amide II, and amide A (N–H stretching) signatures, thus confirming the β-sheet conformation.[47] Importantly, the peak at 1690 cm^{-1} points to an antiparallel β-sheet arrangement[48] of the sheets within the 17H6 fibrils. Evidence of a small amount of α-helical content is also observed at 1545 and 1659 cm^{-1} and is attributed to the α-helical conformation of monomer 17H6 molecules that have not been incorporated into the fibrils.

Atomic force microscopy (AFM) was conducted on samples of the peptide fibrils to determine their height profiles. Figure 2a shows an AFM height image of 17H6

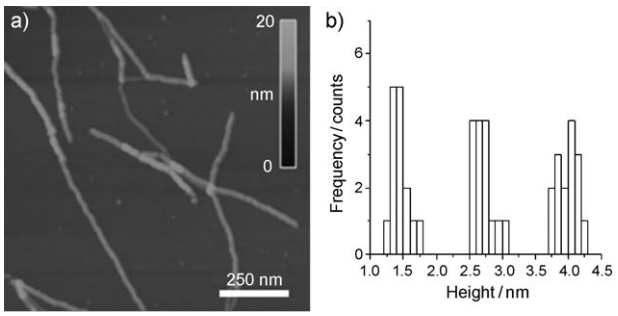

Figure 2. a) AFM height image of 17H6 fibrils. b) Frequency distribution chart of fibril heights obtained from sectional analysis on AFM image in (a).

fibrils. As with TEM, well-defined fibril morphology was observed in AFM. A height histogram generated from sectional analysis on the micrograph shown in Figure 2a is given in Figure 2b. Discrete vertical steps of (1.4 ± 0.1), (2.7 ± 0.1), and (4.0 ± 0.1) nm in the height are clearly observed. A less frequent occurrence of larger heights was also observed but, notably, the measured heights are significantly lower than the fibril width measured in TEM. This observation is strongly indicative of a rectangular fibril cross-section as opposed to a cylindrical one, which would yield a height equal to its width (additional AFM height data is shown in the Supporting Information).

The data from the characterization methods described above were combined to build a structural model for the 17H6 fibril. The secondary structure of the polypeptide was established as β-sheet by CD and FTIR spectroscopy, and the β-sheet repeat spacing was quantified as 4.56 Å from the WAXS data. Widths observed in TEM (7.6 nm) are in good agreement with the length of the 22-residue alanine-rich repeat segment AAAQEAAAAQAAAQAEAAQAAQ (7.7 nm) in the β-sheet conformation (3.5 Å per residue). This result suggests that the repeating alanine-rich segment folds over to form antiparallel β-hairpin substructures, which form the width of the fibril, as shown in Figure 3. The antiparallel configuration of the β sheets is corroborated by the presence of a peak at 1690 cm^{-1} in the FTIR spectrum. Hydrophobic interactions and hydrogen bonding are the primary driving forces that cause such assembly in 17H6; hairpin substructures have also been reported for other alanine-rich sequences.[48–50] Hydrophobic interactions promote the exclusion of water and other hydrophilic species by collapse of the hydrophobic alanine residues. Hydrogen bonding within the β sheets stabilizes this structure, which incorporates more 17H6 monomer units in a similar manner and leads to fibril axial fibril growth. When viewed under crossed polarizers in optical microscopy, 17H6 fibrils were found to exhibit a green colored birefringence upon binding to congo red (see Figure S3 in the Supporting Information). These fibrils were also found to bind thioflavin T. The

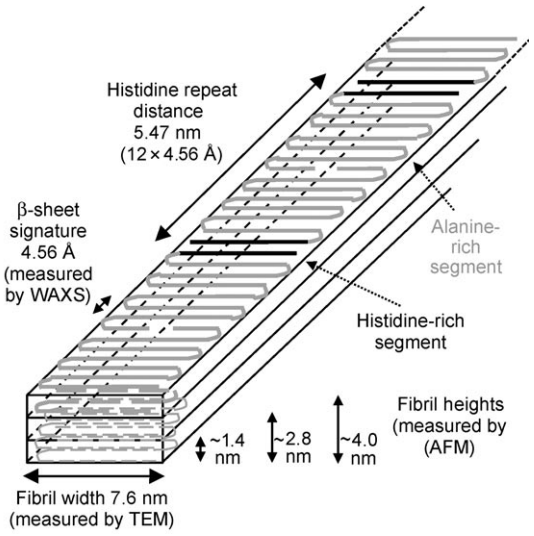

Figure 3. Structural model for 17H6 fibril showing antiparallel β-sheet arrangement of alanine-rich repeat segment (marked in gray) and spatially repeating positively charged histidine patches (marked in black).

combination of these results suggests the presence of a cross-β structural motif,[46] wherein β strands are perpendicular to the fibril growth axis and planes defined by β sheets lie parallel to the fibril growth axis. Two substructures stack vertically to form a bilayer. A rectangular cross-section with a height much smaller than the width thus results as a consequence of this vertical stacking, which is most likely driven by hydrophobic interactions. AFM sectional analyses yield an average height of 1.4 nm for these bilayers; this value corresponds well with the expected height of a bilayer when the side-chain lengths of residues of the alanine-rich sequence are considered. Two or more bilayer substructures may stack laterally to cause fibril vertical growth (observed as multiples of 1.4 nm), although single- and double-layer fibrils occur most frequently. Vertical stacking has been observed previously in other experimental examples of self assembly of alanine-rich sequences.[48] The axial assembly of two hairpins in a head-to-tail manner maximizes hydrophobic contact, and places histidine segments together. Such assembly is supported by an analysis of the average interparticle spacing measured in 17H6-templated nanoparticle arrays (see below). Exclusion of the histidine segments from the interior of the fibril would not result in the observed quantization of the interparticle spacing along the fibril length and is thus ruled out. Electrostatic repulsion between histidine segments contributes marginally to the opposition of such assembly, but hydrogen bonding and hydrophobic interactions dominate, and bury the C termini of polypeptide molecules together. The histidine-rich segment is thus arranged regularly along the fibril length with a spatial periodicity of 5.47 nm (12 × 4.56 Å). These regularly repeating, positively charged histidine patches represent the most promising feature of this nanoarchitecture, as they can be utilized for the controlled placement of oppositely charged inorganic nanoparticles.

Nanogold was chosen as a model particle system for the construction of 17H6 templated one-dimensional arrays as the citrate-reduction methodology to produce negatively charged nanoparticles is well-established.[51] The simultaneous addition of a reducing agent (sodium citrate) and a stabilizing ligand (sodium 3-mercaptopropionate, MPA-Na) allowed the production of 2–3 nm Au nanoparticles.[38,52] These nanoparticles bear a negative charge in solution, owing to the dissociation of MPA-Na. 17H6 fibrils were mixed together with an excess of gold nanoparticles and stirred overnight. The gold nanoparticles became immobilized on the 17H6 fibrils, thus neutralizing the charge on the positively charged histidine patches, and the fibril–particle assemblies precipitated from the solution. Figure 4a shows a

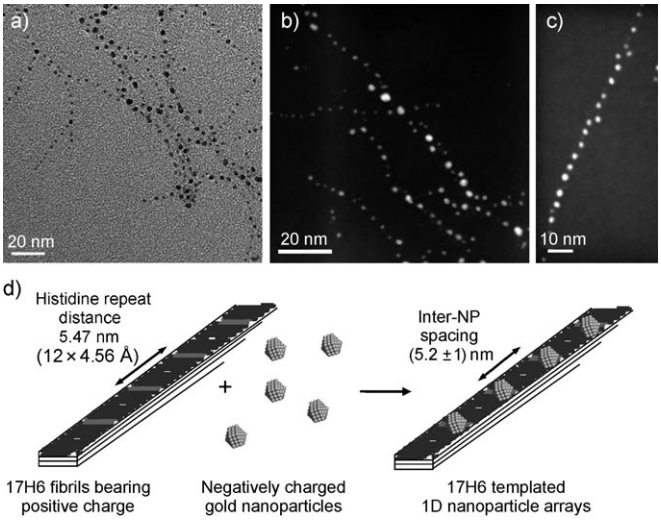

Figure 4. a) BF TEM image of 17H6 templated 1D gold nanoparticle arrays; b) HAADF-STEM image showing the high fidelity of the 2 nm gold nanoparticles to the 17H6 fibrils; c) HAADF-STEM image showing controlled axial nanoparticle positioning with (5.2 ± 1) nm interparticle spacing; d) mechanism for electrostatic assembly of negatively charged gold nanoparticles on positively charged histidine patches in 17H6 fibrils.

BF TEM image of gold nanoparticle arrays on 17H6 fibrils. The gold nanoparticles bind to 17H6 fibrils with a high fidelity, and successful templating is observed over hundreds of nanometers in length. The fibrils themselves are not stained and are hence invisible because of their lower electron density. A statistical analysis of inter-nanoparticle spacing on this image yields an average interparticle spacing of (5.5 ± 1.2) nm, which is in good agreement with the spacing between histidine segments proposed in the model in Figure 3. The large standard deviations associated with the measurement of inter-nanoparticle spacing arise from convolutions that arise from particle size polydispersity and the measurement's sensitivity to imaging artifacts such as focus and astigmatism. Figure 4b,c show high-angle annular dark field scanning transmission electron microscopy (HAADF-STEM) images of 17H6-Au nanoparticle arrays. In HAADF-STEM mode, bright areas on the micrograph correspond to regions of high atomic number, and in our case highlight the gold nanoparticles with a high degree of clarity. The interparticle spacing in Figure 4c was measured to be (5.2 ± 1.0) nm.

Debye theory suggests that the observation of this interparticle spacing implies templating and not merely electrostatically controlled repulsion of particles during assembly.[53] A fibril that possesses an entirely hydrophilic surface that is positively charged would have an interparticle spacing closer to the Debye length of the solutions, as defined by their ionic strengths or close-packed assembly along the mediating nanostructure, as observed in other electrostatic assembly systems.[22] However, the measured average interparticle spacing far exceeds the Debye length ($K^{-1} = 0.51$ nm) of the solutions used for the nanoparticle deposition. Notably, the addition of stoichiometrically higher quantities of gold nanoparticles does not lead to a decrease in interparticle spacing. When all the available histidine patches in a fixed volume of 17H6 fibril solution are satisfied by gold nanoparticles, no further assembly is observed after the addition of a further excess of gold nanoparticles, as all the oppositely charged sites are satisfied and therefore inaccessible. Additionally, variations in the ionic strength of the solutions used during assembly measurably affect the assembly kinetics, as charge-screening results in slower assembly kinetics at higher ionic strengths. This effect illustrates the electrostatically directed binding of the nanoparticles, which not only confirms the validity of the patched-histidine model of 17H6 self-assembly but also suggests the potential of these strategies in bottom–up assembly as shown in Figure 4d. Negatively charged nanoparticles bind to the positively charged histidine patches by electrostatic interactions in solution and become immobilized, thus resulting in one-dimensional nanoparticle arrays. A nanoparticle bound to a histidine patch prevents another from binding to the same patch by electrostatic repulsion.

Modularity is a key advantage of the electrostatic assembly approach as it introduces the flexibility afforded by the host of particle nanoengineering[54] techniques that are presently available, such as ligand exchange. Moreover, this system offers a convenient, bottom–up method of placing nanoparticles at predefined separations in a one-dimensional configuration. These hybrids can then be utilized for the study of fundamental interactions between nanoparticles. Most importantly, the inter-nanoparticle spacing may potentially be tuned by systematic changes in the primary sequence, such as by simply increasing the number of alanine-rich segments in the polypeptide. If it assumed that a similar hierarchical assembly pathway is followed by longer polypeptides with an identical alanine-segment composition, changing the number of alanine-rich repeat segments would control inter-histidine separation and, consequently, the templated inter-nanoparticle spacing. Control over inter-nanoparticle spacing at such length scales is at the limit of state-of-the-art lithographic capability but is potentially accessible using this polypeptide architecture. Particle immobilization through these methods is not limited to electrostatic interactions; specific affinities towards inorganic materials may be engineered by alteration of the histidine-bearing N terminus to incorporate different types of binding groups and functional epitopes.

In conclusion, we have demonstrated the ability of an alanine-rich polypeptide to template nanoparticle assembly by the assembly of the polypeptide into β-sheet fibrils. Electron microscopy, X-ray scattering, FTIR, and atomic force microscopy indicate the assembly of the polypeptide into a unique molecular architecture with spatially repeating positively charged patches. These positively charged patches permit the immobilization of negatively charged gold nanoparticles through complementary electrostatic interactions by a solution-phase assembly process. This system can be utilized for the construction of one-dimensional arrays of different nanoparticle types and offers a potential method for modulating inter-nanoparticle spacing by polypeptide sequence programming. It is expected that these nanoparticle arrays would be useful for studying quantum mechanical behavior in nanoparticle interactions. These one-dimensional nanoparticle arrays would also be promising candidates as materials for the construction of nanoscale optoelectronic devices.

Received: March 25, 2009
Revised: July 14, 2009
Published online: August 18, 2009

Keywords: bottom–up fabrication · gold · nanostructures · peptides · self-assembly

[1] A. N. Shipway, E. Katz, I. Willner, *ChemPhysChem* **2000**, *1*, 18.
[2] Z. Y. Tang, N. A. Kotov, *Adv. Mater.* **2005**, *17*, 951.
[3] E. Braun, Y. Eichen, U. Sivan, G. Ben-Yoseph, *Nature* **1998**, *391*, 775.
[4] I. S. Jacobs, C. P. Bean, *Phys. Rev.* **1955**, *100*, 1060.
[5] C. Petit, V. Russier, M. P. Pileni, *J. Phys. Chem. B* **2003**, *107*, 10333.
[6] W. Gotschy, K. Vonmetz, A. Leitner, F. R. Aussenegg, *Opt. Lett.* **1996**, *21*, 1099.
[7] L. A. Sweatlock, S. A. Maier, H. A. Atwater, J. J. Penninkhof, A. Polman, *Phys. Rev. B* **2005**, *71*, 235408.
[8] W. Rechberger, A. Hohenau, A. Leitner, J. R. Krenn, B. Lamprecht, F. R. Aussenegg, *Opt. Commun.* **2003**, *220*, 137.
[9] T. Atay, J. H. Song, A. V. Nurmikko, *Nano Lett.* **2004**, *4*, 1627.
[10] R. de Waele, A. F. Koenderink, A. Polman, *Nano Lett.* **2007**, *7*, 2004.
[11] S. A. Maier, M. L. Brongersma, P. G. Kik, S. Meltzer, A. A. G. Requicha, H. A. Atwater, *Adv. Mater.* **2001**, *13*, 1501.
[12] S. A. Maier, P. G. Kik, H. A. Atwater, S. Meltzer, E. Harel, B. E. Koel, A. A. G. Requicha, *Nat. Mater.* **2003**, *2*, 229.
[13] M. Quinten, A. Leitner, J. R. Krenn, F. R. Aussenegg, *Opt. Lett.* **1998**, *23*, 1331.
[14] P. M. Ajayan, S. Iijima, *Nature* **1993**, *361*, 333.
[15] M. Aslam, R. Bhobe, N. Alem, S. Donthu, V. P. Dravid, *J. Appl. Phys.* **2005**, *98*, 074311.
[16] B. L. Frankamp, A. K. Boal, V. M. Rotello, *J. Am. Chem. Soc.* **2002**, *124*, 15146.
[17] R. Shenhar, T. B. Norsten, V. M. Rotello, *Adv. Mater.* **2005**, *17*, 657.
[18] G. M. Whitesides, B. Grzybowski, *Science* **2002**, *295*, 2418.
[19] I. W. Hamley, *Angew. Chem.* **2003**, *115*, 1730; *Angew. Chem. Int. Ed.* **2003**, *42*, 1692.
[20] A. P. Alivisatos, K. P. Johnsson, X. G. Peng, T. E. Wilson, C. J. Loweth, M. P. Bruchez, P. G. Schultz, *Nature* **1996**, *382*, 609.
[21] J. W. Zheng, P. E. Constantinou, C. Micheel, A. P. Alivisatos, R. A. Kiehl, N. C. Seeman, *Nano Lett.* **2006**, *6*, 1502.
[22] M. G. Warner, J. E. Hutchison, *Nat. Mater.* **2003**, *2*, 272.
[23] Y. Y. Pinto, J. D. Le, N. C. Seeman, K. Musier-Forsyth, T. A. Taton, R. A. Kiehl, *Nano Lett.* **2005**, *5*, 2399.

[24] J. Sharma, Y. G. Ke, C. X. Lin, R. Chhabra, Q. B. Wang, J. Nangreave, Y. Liu, H. Yan, *Angew. Chem. Int. Ed.* **2008**, *47*, 5157.
[25] R. A. McMillan, C. D. Paavola, J. Howard, S. L. Chan, N. J. Zaluzec, J. D. Trent, *Nat. Mater.* **2002**, *1*, 247.
[26] S. Howorka, *J. Mater. Chem.* **2007**, *17*, 2049.
[27] M. H. Hu, L. P. Qian, R. P. Brinas, E. S. Lymar, J. F. Hainfeld, *Angew. Chem.* **2007**, *119*, 5203; *Angew. Chem. Int. Ed.* **2007**, *46*, 5111.
[28] E. Dujardin, C. Peet, G. Stubbs, J. N. Culver, S. Mann, *Nano Lett.* **2003**, *3*, 413.
[29] K. T. Nam, *Science* **2008**, *322*, 44.
[30] M. G. Ryadnov, D. N. Woolfson, *J. Am. Chem. Soc.* **2004**, *126*, 7454.
[31] T. Scheibel, R. Parthasarathy, G. Sawicki, X. M. Lin, H. Jaeger, S. L. Lindquist, *Proc. Natl. Acad. Sci. USA* **2003**, *100*, 4527.
[32] A. Aggeli, I. A. Nyrkova, M. Bell, R. Harding, L. Carrick, T. C. B. McLeish, A. N. Semenov, N. Boden, *Proc. Natl. Acad. Sci. USA* **2001**, *98*, 11857.
[33] M. S. Lamm, K. Rajagopal, J. P. Schneider, D. J. Pochan, *J. Am. Chem. Soc.* **2005**, *127*, 16692.
[34] K. Rajagopal, J. P. Schneider, *Curr. Opin. Struct. Biol.* **2004**, *14*, 480.
[35] D. N. Woolfson, M. G. Ryadnov, *Curr. Opin. Chem. Biol. Mod. Sys./Biopolym.* **2006**, *10*, 559.
[36] S. R. Whaley, D. S. English, E. L. Hu, P. F. Barbara, A. M. Belcher, *Nature* **2000**, *405*, 665.
[37] L. T. Yu, I. A. Banerjee, H. Matsui, *J. Am. Chem. Soc.* **2003**, *125*, 14837.
[38] M. S. Lamm, N. Sharma, K. Rajagopal, F. L. Beyer, J. P. Schneider, D. J. Pochan, *Adv. Mater.* **2008**, *20*, 447.
[39] D. Aili, K. Enander, L. Baltzer, B. Liedberg, *Nano Lett.* **2008**, *8*, 2473.
[40] X. Y. Fu, Y. Wang, L. X. Huang, Y. L. Sha, L. L. Gui, L. H. Lai, Y. Q. Tang, *Adv. Mater.* **2003**, *15*, 902.
[41] L. S. Li, S. I. Stupp, *Angew. Chem.* **2005**, *117*, 1867; *Angew. Chem. Int. Ed.* **2005**, *44*, 1833.
[42] R. Djalali, Y. Chen, H. Matsui, *J. Am. Chem. Soc.* **2002**, *124*, 13660.
[43] R. Djalali, Y. F. Chen, H. Matsui, *J. Am. Chem. Soc.* **2003**, *125*, 5873.
[44] R. S. Farmer, L. M. Argust, J. D. Sharp, K. L. Kiick, *Macromolecules* **2006**, *39*, 162.
[45] A. Top, K. L. Kiick, C. J. Roberts, *Biomacromolecules* **2008**, *9*, 1595.
[46] M. R. Sawaya, S. Sambashivan, R. Nelson, M. I. Ivanova, S. A. Sievers, M. I. Apostol, M. J. Thompson, M. Balbirnie, J. J. W. Wiltzius, H. T. McFarlane, A. O. Madsen, C. Riekel, D. Eisenberg, *Nature* **2007**, *447*, 453.
[47] T. Miyazawa, E. R. Blout, *J. Am. Chem. Soc.* **1961**, *83*, 712.
[48] T. Yu, J. Z. Bai, Z. Guan, *Angew. Chem.* **2009**, *121*, 1117; *Angew. Chem. Int. Ed.* **2009**, *48*, 1097.
[49] J. M. Smeenk, M. B. J. Otten, J. Thies, D. A. Tirrell, H. G. Stunnenberg, J. C. M. van Hest, *Angew. Chem.* **2005**, *117*, 2004; *Angew. Chem. Int. Ed.* **2005**, *44*, 1968.
[50] H. D. Nguyen, A. J. Marchut, C. K. Hall, *Protein Sci.* **2004**, *13*, 2909.
[51] J. Turkevich, P. C. Stevenson, J. Hillier, *Discuss. Faraday Soc.* **1951**, *11*, 55.
[52] T. Yonezawa, T. Kunitake, *Colloid Surf. A* **1999**, *149*, 193.
[53] J. Israelachvili, *Intermolecular and Surface Forces*, 2nd ed., Academic Press Ltd., San Diego, **1991**.
[54] F. Caruso, *Adv. Mater.* **2001**, *13*, 11.

